J Mater Sci (2008) 43:3931–3937
DOI 10.1007/s10853-007-2371-6

Microstructure and Vickers hardness of Co/Cu multilayers fabricated by electrodeposition

Y. Kaneko · H. Sakakibara · S. Hashimoto

Received: 7 July 2007 / Accepted: 3 December 2007 / Published online: 21 March 2008

Abstract In order to investigate thermal stability of Co/Cu multilayers fabricated by electrodeposition, Vickers hardness tests and microstructure observations were conducted on both as-deposited and annealed Co/Cu multilayers having a layer thickness of 100 nm. The multilayers were annealed at temperatures ranging from 473 to 1,273 K for 1 h. It is confirmed that even after the annealing at 1,023 K, the multilayer maintained the high hardness (Hv231) which was comparative to that of the as-deposited Co/Cu multilayer. When the annealing temperature was higher than 1,073 K, the hardness decreased rapidly with increasing temperature. Scanning electron microscopy (SEM) observation revealed that the multilayered structures were still maintained without any layer damages after the annealing at the temperatures less than 873 K. At the cross sections of the Co/Cu multilayers annealed at $T > 923$ K, several copper layers were fragmented. The layered structure finally disappeared by the annealing at 1,273 K. The rapid decrease in the hardness at $T > 1{,}073$ K is simply understood from the annihilation of the Co/Cu interfaces.

Introduction

Due to inhibiting dislocation movements, grain boundaries (GBs) play an important role on strength of metallic materials. In a metallic material with high-density GBs, the strength will increase in accordance with the Hall-Petch relation. The high-density GBs are normally produced by grain refinement which has been realized in the gas-condensation method [1] and the severe plastic deformation [2]. The ultrafine-grained materials produced by an equal channel angular pressing have actually revealed high yield strength [3–5].

Similar strengthening is expected in a multilayered structure which is composed from alternate stacks of two different metallic layers. It can be said that the multilayer has one-dimensional fine-grained structure. Hence, thinning of component metallic layers will lead to the strength enhancement. Indeed, the multilayered structures have been exhibited high tensile strength [6, 7] and hardness [8–12]. Such investigations on the mechanical properties of multilayers have been conducted mostly on the Ni/Cu multilayers. This may be because the fabrication of the Ni/Cu multilayer by electrodepositing technique had been established in several studies focusing on magnetic properties of multilayered structures [13, 14]. However, because the Ni–Cu alloy system is an all-proportional solid solution, thermal stability of the Ni/Cu multilayers is poor: the component Ni and Cu layers will become a Ni–Cu alloy at elevated temperature.

The electrodeposition technique can produce a Co/Cu multilayered film, as well as the Ni/Cu multilayer. For the electrodeposited Co/Cu multilayers, scientific interests have concentrated on the magnetic properties [14–21]. On the other hand, the mechanical properties have not been reported in the Co/Cu multilayers yet, as far as we know. Unlike the Ni–Cu binary system, the Co and Cu phases separate from each other even at elevated temperature. Therefore, it is quite likely that the Co/Cu multilayered structure exhibits excellent thermal stability.

In the present study, the authors fabricated the Co/Cu multilayers on copper substrate by the electrodepositing

Y. Kaneko (✉) · H. Sakakibara · S. Hashimoto
Department of Intelligent Materials Engineering, Faculty of Engineering, Osaka City University, Sugimoto 3-3-138, Sumiyoshi-ku, Osaka 558-8585, Japan
e-mail: kaneko@imat.eng.osaka-cu.ac.jp

technique. The Co/Cu multilayers were annealed at various temperatures. The thermal stability of the Co/Cu multilayer was estimated by Vickers hardness test. Annealing temperature dependence of the hardness was discussed from morphologies of the component layers which were observed by scanning electron microscopy (SEM).

Experimental procedure

The Co/Cu multilayers were fabricated on polycrystalline copper substrates by an electrodepositing technique. Before the electrodeposition, the copper substrates were annealed at 1,073 K for 1 h in vacuum and then polished mechanically and electrolytically. The electrodeposition were conducted in an aqueous solution containing $CoSO_4 \cdot 7H_2O$ (300 g/L), $CuSO_4 \cdot 5H_2O$ (1.9 g/L) and H_3BO_3 (30 g/L). Since ionization tendency of cobalt is higher than that of copper, a chemical composition of an electrodeposit depends on an electric potential applied to the substrate. At the potential range where the cathodic current is almost zero, copper is exclusively deposited. On the other hand, copper and cobalt atoms would be deposited simultaneously at high-cathodic potential region. In order to obtain a Co-rich deposit at the high-cathodic potential region, the copper sulfate content in the solution was set at significantly low in comparison with the cobalt sulfate. In the present study, the Co-rich and Cu layers were deposited at −1,000 and −250 mV vs. SHE, respectively. By applying two different potentials alternately using the Hokuto-Denko HA151 potensiostat to which a computer was equipped, we fabricated the Co/Cu multilayers on the copper substrate. The thickness of the deposited layer was controlled in accordance with the measured electric charge during the electrodeposition: the electric potential was switched to the other one when a total electric charge became a predetermined value. The calculations of the predetermined electric charges were based on the Faraday's law, assuming that the current efficiency was 80%. A ratio of Co layer thickness to Cu one was 1:1 in the present study. The thickness of each layer was 100 nm.

In order to investigate thermal stability, the Co/Cu multilayers were annealed at temperatures from 473 to 1,273 K for 1 h. Thereafter, values of Vickers hardness were measured at room temperature. Total multilayer thickness was 1 μm for all the Co/Cu multilayers prepared for the hardness tests. The hardness tests were carried out using Shimadzu DUH-W201 tester, which can record displacement of an indenter during the test. The hardness was estimated from an indentation depth. The hardness tests were conducted under the condition that the Co/Cu multilayers were not removed from the copper substrates. The indentation force was set at 4.9 mN in the present study. We measured the hardness ten times for each specimen.

Cross sections of the Co/Cu multilayers were observed with the JEOL JSM-6500F field-emission SEM and the JEOL JEM-2100 TEM. The Co/Cu multilayers prepared for the cross section observations had the total thickness of 2 μm, and the surfaces were covered with thick copper films which were electrodeposited in a copper sulfate aqueous solution. For the SEM observation, the cross sections were polished with 1 μm and 3 μm diamond pastes to identify the individual layers. The Co/Cu multilayer for the TEM observation was deposited on a copper single crystal having $(1\bar{1}1)$ surface. This is because the TEM observation direction lying in the Co/Cu interface plane has a low Miller index to obtain a simple electron diffraction pattern. In the present study, the Co/Cu multilayer was cut parallel to $(\bar{1}12)$ plane which is perpendicular to the $(1\bar{1}1)$ surface. Microstructures of the Co/Cu multilayers were investigated by the X-ray diffraction analysis (XRD) using a cobalt target.

Results and discussion

Microstructure of the as-deposited multilayer

A simple electrodeposition in the above aqueous solution were first conducted at a static potential ranging from −1,100 to 0 mV vs. SHE. Figure 1 shows dependence of deposit composition on the applied potential. At the potential range higher than −400 mV vs. SHE, only pure copper was deposited. On the other hand, the deposits contained both copper and cobalt at the potential less than −500 mV vs. SHE. Even at significantly low potential, pure cobalt could not be obtained. Accordingly, cobalt layers in a Co/Cu multilayer, which was electrodeposited at −1,000 mV vs. SHE, actually was Co-4at.% Cu alloy.

In order to clarify lattice structures and orientation relationship between the Co and Cu layers, a cross section of as-deposited Co/Cu multilayer having the 100 nm layer thickness was observed by TEM. Figure 2 shows a STEM photograph, an EDX image, and an electron diffraction pattern of the Co/Cu sample cut parallel to $(\bar{1}12)$ plane. Although an identification of each layer is difficult in the STEM photograph, the lamellar structure is confirmed in the EDX image. A ratio of the Cu to Co layer thickness measured in this multilayer was approximately 1:1, which was in accordance with the predetermined thicknesses. In the electron diffraction pattern, we can notice that some spots split into two along a radial direction. The spot splitting is attributed to reflections from the Cu and fcc-Co layers which have different lattice parameters. Accordingly, from the diffraction pattern, it is found that the

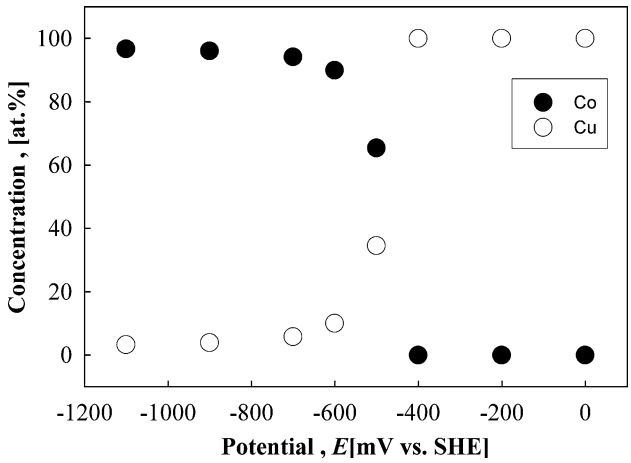

Fig. 1 Dependence of chemical composition of electrodeposits on the applied potential

lattice structure of the Co layer was the fcc lattice and the Cu and Co layers had almost the same crystallographic orientation. Moreover, as indicated in Fig. 2, the splitting spots were deviated also along a circumferential direction by 1.5°, in addition to the deviation along the radial direction. This result implies that the orientation of the Cu

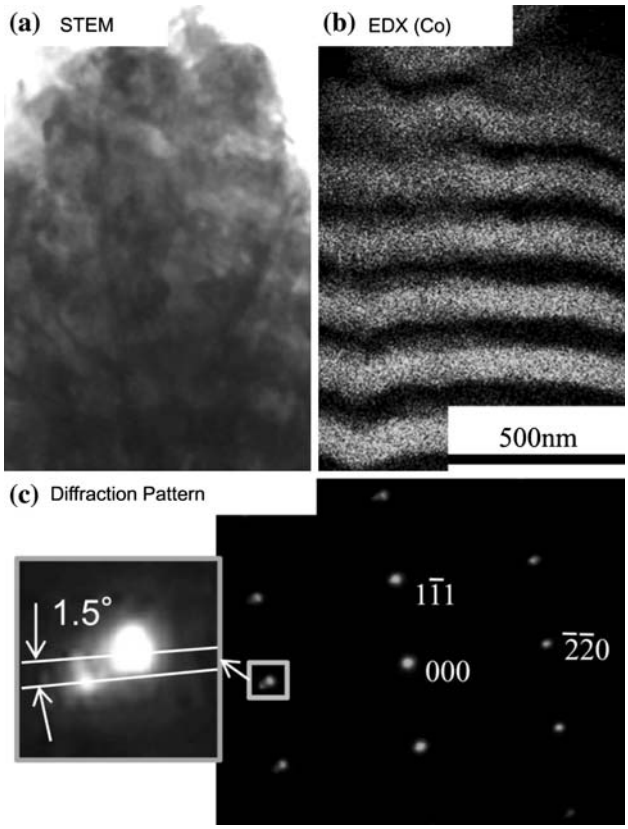

Fig. 2 (**a**) STEM image, (**b**) EDX image, and (**c**) electron diffraction pattern of the cross section of the as-deposited Co/Cu multilayer formed on a copper single crystal having $(1\bar{1}1)$ surface. The thin foil was cut parallel to $(\bar{1}12)$ plane of the substrate

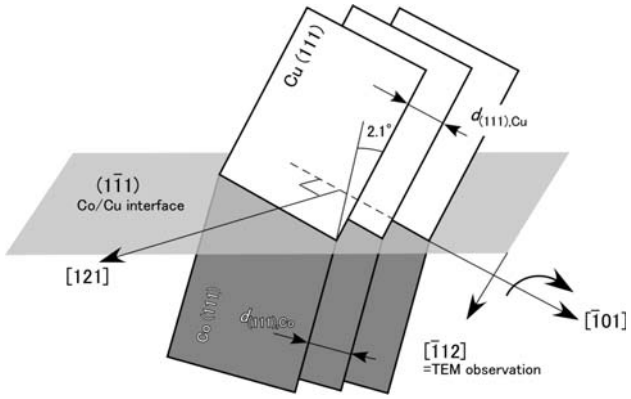

Fig. 3 Schematic model of (111) planes in the cobalt and copper layers. The copper lattice rotates around $[\bar{1}01]$ axis by 2.1° to maintain continuity of the (111) planes of both layers across Co/Cu interface

layers was slightly different from that of the Co layers. In the HREM observation of the Ni/Cu multilayer having very short layer thicknesses (h_{Cu} = 1.4 nm and h_{Ni} = 2.5 nm) [18], a lattice plane across layers has not been straight and the Ni/Cu interfaces have possessed coherent structures. Lattice mismatch at the Ni/Cu interface was relaxed not fully by misfit dislocations, but partially by lattice rotation. A part of the lattice mismatch at the present Co/Cu interface was possibly relaxed by the lattice rotation in the same manner.

The authors considered a lattice rotation model which can provide a coherent lattice plane at the $(1\bar{1}1)$ Co/Cu interface. Since {111} planes have the smallest lattice spacing ($d_{(111)Cu}$ = 2.555 Å and $d_{(111)Co}$ = 2.523 Å), the lattice continuity between the (111) planes of the Cu and Co layers was treated. The Cu crystal is supposed to rotate around $[\bar{1}01]$ axis such that the individual (111) planes are continuous across the interface, as schematically shown in Fig. 3. The required rotation around the $[\bar{1}01]$ axis was about 2.1°. Under this orientation relation, a dihedral angle between the $(\bar{1}\bar{1}1)$ planes of the Cu and Co layers is calculated to be 1.7°. This value is almost identical to the circumferential deviation angle (= 1.5°) between the splitting spots. Consequently, the slight orientation difference between the Cu and Co layers could be interpreted in terms of the partial accommodation of lattice mismatch by the lattice rotation. It is noted that the Co/Cu interface is not fully coherent in this model. Although lattice mismatch along [121] direction is accommodated by the lattice rotation around $[\bar{1}01]$ axis, lattice mismatch along $[\bar{1}01]$ direction still remains.

Vickers hardness

Dependence of the Vickers hardness on annealing temperature is shown in Fig. 4. The Vickers hardness of the

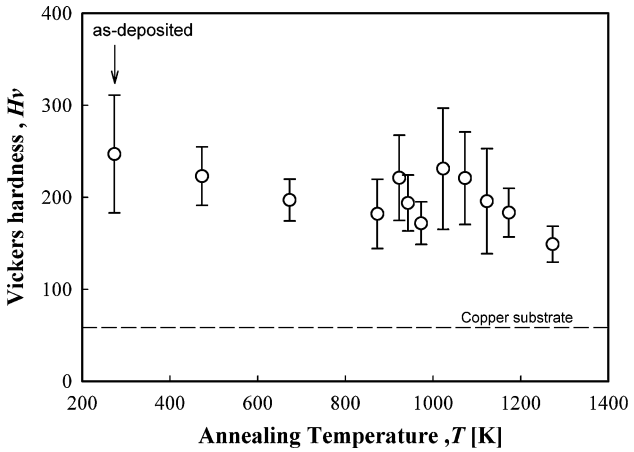

Fig. 4 Dependence of Vickers hardness on the annealing temperature in the Co/Cu multilayers having 100 nm layer thickness

as-deposited Co/Cu multilayer was Hv246 which was higher than that of the as-deposited Ni/Cu multilayer with the same layer thickness [10]. The hardness of the Co/Cu multilayer gradually decreased with increasing temperature at $T \leq 873$ K. At the temperature near 1,023 K, a local increase in the hardness is recognized. The local maximum of the hardness was Hv231. When the temperature was higher than 1,073 K, the hardness decreased rapidly with increasing temperature. Consequently, it is evident that even after the annealing at the 1,023 K, the Co/Cu multilayer maintained the high hardness which was comparative to that of the as-deposited Co/Cu multilayer. On the other hand, the hardness of the Ni/Cu multilayer decreased rapidly at the temperatures more than 623 K [22]. This is because the Ni/Cu multilayered structure disappeared due to the fact that the Ni and Cu layers are easily mixed with each other at the elevated temperature.

Microstructures of the annealed multilayers

The cross sections of the Co/Cu multilayers annealed at various temperatures are presented in Fig. 5. The total thickness of the observed multilayers was about 2 μm. The grooved areas induced by the diamond polishing roughly correspond to the Co phase. It should be noted that the amount of the Co layer in the as-deposited multilayer seems smaller than the predetermined one, in spite of the fact that the ratio of the Cu to Co layer thickness was about 1:1 in the EDX analysis using the TEM. It is probable that the Co phase was not completely removed from the cross section by the diamond polishing.

The SEM observations revealed that the Co and Cu layers separated from each other still after the annealing at 1,073 K. This result is consistent with the prediction based on a phase diagram of Co–Cu binary system [23]. After the annealing at the temperatures less than 873 K, the multilayered structures were still maintained without any layer damage. At the cross sections of the Co/Cu multilayers annealed at $T \geq 923$ K, we can see several fragmented copper layers. The degree of the fragmentation increased with the increasing annealing temperature. Finally, the layered structure completely disappeared by the annealing at 1,273 K. The rapid decrease in the hardness at $T \geq 1{,}073$ K is simply understood from the annihilation of the Co/Cu interfaces which can be barriers against dislocation passages.

At the multilayers annealed at 923 and 1,023 K, there are many small particles existing inside the Co layers. These small particles are considered as the copper-rich phase precipitated during cooling period after the isothermal annealing. In the Co–Cu alloy system, copper solubility in the cobalt-rich phase increases with increasing

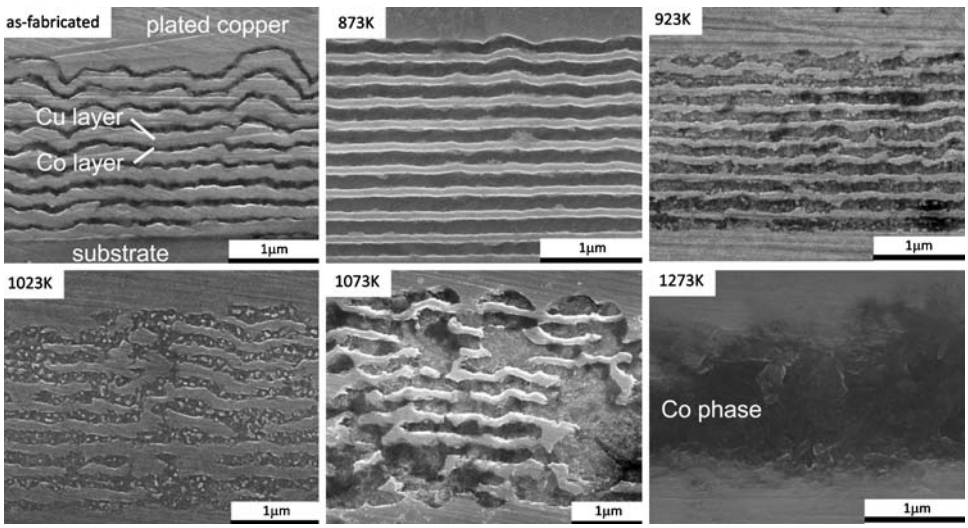

Fig. 5 SEM photographs showing the cross sections of the Co/Cu multilayers which were annealed at various temperatures for 1 h

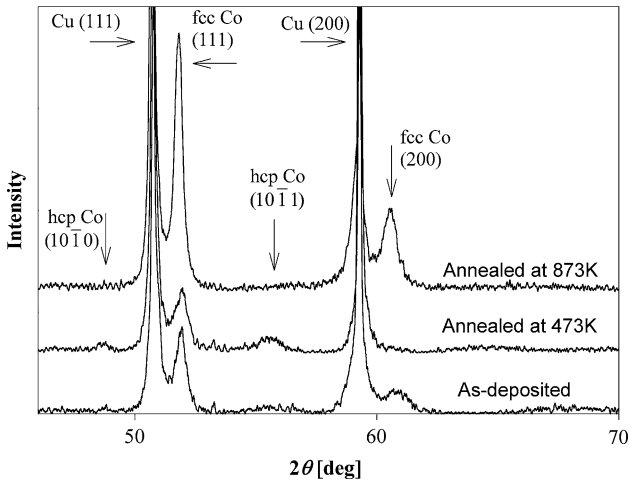

Fig. 6 X-ray diffraction patterns of the as-deposited Co/Cu multilayers and those annealed at 473 and 873 K

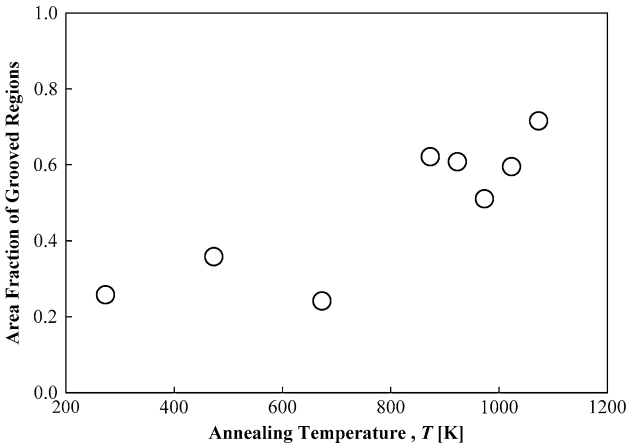

Fig. 7 Annealing temperature dependence of the fraction of the Co phase in the Co/Cu multilayered structure. The fraction was determined by the measurement of the grooved areas observed at the polished cross sections

temperature [23]. Therefore, the copper content in the Co layer at high temperature should exceed equilibrium content at room temperature. Since the specimens were cooled in a furnace after the annealing, a cooling rate was not rapid. It is likely that the excess copper atoms in the Co layers were precipitated during the cooling period. The local hardness increase seen near 1,023 K in Fig. 4 can be interpreted in terms of the precipitation hardening of the small particles.

Figure 6 shows X-ray diffraction patterns of the as-deposited and the annealed Co/Cu multilayers having 100 nm layer thickness. The diffraction patterns were measured at the multilayers being deposited on the copper substrates, thus strong intensity of Cu peaks come partially from the copper substrates. Since the Bragg angles of (0002) and (111) peaks from hcp- and fcc-cobalt are almost the same, the identification of lattice structure from these peaks was difficult. In the as-deposited multilayer, the diffraction peaks of the Co layers were from the fcc-cobalt. The peaks from the hcp-cobalt, such as $(10\bar{1}0)$ and $(10\bar{1}1)$, were very weak. The structure of the Co layers in the as-deposited multilayer having 100 nm layer thickness was the fcc lattice, although a stable structure is the hcp lattice at $T < 695$ K.

At the multilayer annealed at 473 K, small $(10\bar{1}0)$ and $(10\bar{1}1)$ peaks from the hcp-cobalt are recognized. On the contrary, the (200) peak of the fcc-cobalt almost disappeared. Hence, a part of the fcc-cobalt in the as-deposited multilayer was transformed to the hcp lattice due to the annealing. Since the cobalt phase has a phase transformation temperature at 695 K, the diffraction peaks from the hcp lattice disappeared again at the annealing at 873 K. In Fig. 4, the plots at 473 and 673 K corresponded to the results of the multilayers containing the hcp-cobalt phase. However, there is no significant difference in the hardness from the other multilayers without the hcp-cobalt phase.

According to a layer fragmentation model based on GB energy [24], the Co layer should be separated at GBs existing inside the Co layers. However, in the present study, the Cu layers were fragmented as seen in Fig. 5. From the SEM images of the cross sections, the authors measured the amount of the grooved areas corresponding to the Co phase in the multilayered structures. Figure 7 shows the fractions of the grooved area in the multilayered structure, which are plotted against the annealing temperature. The fraction of the grooved areas (the Co phase) increased with increasing annealing temperature. At high temperatures ($T > 800$ K), the amount of the Cu phase was reduced apparently. This result means that copper atoms of the multilayered structure moved to the copper substrate and the protecting copper film. Solubility of both Cu in Co phase and Co in Cu phase increases with increasing temperature [23]. Hence, in the Co/Cu multilayer, Cu atoms would move from Cu layers to Co layers by means of diffusion. The Cu atoms in the outermost Co-rich layer can be absorbed in the copper substrate. This movement of the Cu atoms from the multilayer to the copper substrate may cause the reduction of the Cu phase in the multilayer. Finally, the Cu phase would be annihilated in the multilayered structure as shown in Fig. 5 (1,273 K). Interface energy in the multilayered structure may be one of driving forces for the copper atom movement, because total area of the Co/Cu interface is reduced if the Cu layers are fragmented.

In order to investigate the effect of neighboring metal on the layer fragmentation, the authors prepared the Co/Cu multilayers deposited on cobalt substrates. Surface of the Co/Cu multilayer was covered with a thick cobalt film by

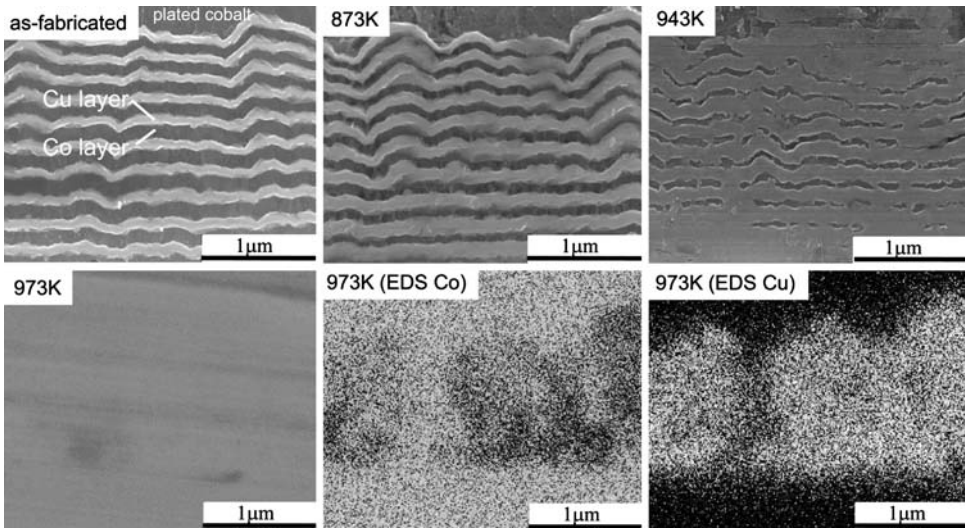

Fig. 8 SEM and ESD images of the cross sections of the annealed Co/Cu multilayers which were deposited on cobalt substrates and were covered with thick cobalt film

electrodeposition. These multilayers were annealed at temperatures from 873 to 973 K, and then cross sections were observed with the SEM in the same manner. The cross sections of the multilayers with the cobalt substrate are presented in Fig. 8. The cross section of the multilayer annealed at 973 K was flattened by mechanical polishing for the EDS analysis. It is found that under the 943 K annealing condition the fragmentation of the Co layers occurred, while the Cu layers were fragmented on the multilayers with the copper substrate. The multilayered structure disappeared in the annealing at 973 K. Hence, the Co atoms in the multilayers certainly moved to the adjacent cobalt substrate and the thick cobalt film. Consequently, the fragmentation process of the component layers—which gives rise to the degradation of strength—was strongly affected by the material neighboring the Co/Cu multilayer. The fragmentation model based on the difference between the GB energies [24] was difficult to be adapted for the present experimental results.

It should be pointed out that the thermal stability of the multilayer depended on the material neighboring the multilayer: the multilayer fabricated on the Co and the Cu substrates disappeared at 973 and 1,273 K, respectively. In the case of the Co substrate, the multilayer disappearance should attribute to absorption of the Co atoms existing in the outermost Cu-rich layer into the Co substrate (or into the thick Co film). This idea is consistent with the result that the degree of fragmentation of the outermost Co-rich layer was more noticeable than that of the layers existing at central site of the multilayer as seen in Fig. 8 (943 K). Here, the authors considered the diffusion of Co and Cu atoms in Cu and Co matrices, respectively. The diffusion coefficients calculated for the Co atoms in the Cu matrix and the Cu atoms in the Co matrix at 973 K are 1.63×10^{-12} cm^2/s and 1.73×10^{-15} cm^2/s, respectively [23]. From the calculated diffusion coefficients, we can deduce a simple model that the absorption velocity of the Co atoms existing in the outermost Cu-rich layer into the Co substrate should be higher than that of the Cu atoms in the outermost Co-rich layer into the Cu substrate. Accordingly, the difference in the thermal stabilities could be understood from the diffusivities of the Co and Cu atoms in the outermost layers.

Conclusions

1. Annealing temperature dependence of the Vickers hardness was investigated on the Co/Cu multilayer with 100 nm layer thickness. The hardness gradually decreased with increasing temperature at $T < 873$ K. At the temperature near 1,023 K, a local maximum in the hardness (Hv231) was recognized. It is thus confirmed that even after the annealing at 1,023 K, the Co/Cu multilayer maintained the high hardness which was comparative to that of the as-deposited Co/Cu multilayer. When the temperature was more than 1,073 K, the hardness decreased rapidly with increasing temperature.
2. After the annealing at temperatures less than 873 K, the multilayered structures were still maintained without any layer damage. At the cross sections of the Co/Cu multilayers annealed at $T > 923$ K, several copper layers were fragmented. The degree of the fragmentation increased with the increasing annealing temperature. Finally, the layered structure completely disappeared by the annealing at 1,273 K. The rapid decrease in the hardness at $T > 1{,}073$ K is simply understood from the annihilation of the Co/Cu interfaces.

3. In order to investigate the effect of the neighboring material on the layer fragmentation, the Co/Cu multilayers covered with the cobalt were annealed at various temperatures. It is found that at the 943 K annealing condition the fragmentation of the Co layers occurred, while the Cu layers were fragmented in the multilayers with the copper substrate. Hence, the fragmentation process of the component layers—which gives rise to the degradation of strength—was strongly affected by the material neighboring the Co/Cu multilayer.

Acknowledgements The authors thank N. Uchida and N. Satoh (Osaka City University) for helping the TEM observations of the multilayers. This work was financially supported by the MEXT Grants-In-Aid for Scientific Research (#16760573).

References

1. Gleiter H (1989) Prog Mater Sci 33:223
2. Valiev RZ, Islamgaliev RK, Alexandrov IV (2000) Prog Mater Sci 45:103
3. Valiev RZ, Kozlov EV, Ivanov YF, Lian J, Nazarov AA, Baudelet B (1994) Acta Metall Mater 42:2467
4. Horita H, Fujinami T, Nemoto M, Langdon TG (2001) J Mater Process Technol 117:288
5. Vinogradov A, Hashimoto S, Kopylov VI (2003) Mater Sci Eng A 355:277
6. Menezes S, Anderson DP (1990) J Electrochem Soc 137:440
7. Tench DM, White JT (1991) J Electrochem Soc 138:3757
8. Simunovich D, Schlesinger M, Snyder DD (1994) J Electrochem Soc 141:L10
9. Clemens BM, Kung H, Barnett SA (1999) MRS Bull 24:20
10. Kaneko Y, Mizuta Y, Nishijima Y, Hashimoto S (2005) J Mater Sci 40:3231. doi:10.1007/s10853-005-2690-4
11. Misra A, Verdier M, Lu YC, Kung H, Mitchell TE, Nastasi M, Embury JD (1998) Scr Mater 39:555
12. Mckeown J, Misra A, Kung H, Hoagland RG, Nastasi M (2002) Scr Mater 46:593
13. Bennett LH, Swartzendruber LJ, Lashmore DS, Oberle R, Atzmony U, Dariel MP, Waton RE (1989) Phys Rev B 40:4633
14. Bird KD, Schlesinger M (1995) J Electrochem Soc 142:L65
15. Kashiwabara S, Jyoko Y, Hayashi Y (1997) Physica B 239:47
16. Yamada A, Houga T, Ueda Y (2002) J Magn Magn Mater 239:272
17. Weihnacht V, Peter L, Toth J, Padar J, Kerner ZS, Schneider CM, Bakonyi I (2003) J Electrochem Soc 150:C507
18. Cziraki A, Pierron-Bohnes V, Ulhaq-Bouillet C, Toth-Kadar E, Bakonyi I (1998) Thin Solid Films 318:239
19. Peter L, Cziraki A, Poganiy Z, Kupay Z, Uhlemann M, Herrich M, Arnold B, Bauer T, Wetzig K (2001) J Electrochem Soc 148:168
20. Uhlemann M, Gebert A, Herrich M, Krause A, Cziraki A, Schultz L (2003) Electrochim Acta 48:3005
21. Cziraki A, Koteles M, Peter L, Kupay Z, Padar J, Pogany L, Bakonyi I, Uhlemann M, Herrich M, Arnold B, Thomas J, Bauer HD, Wetzig K (2003) Thin Solid Films 433:237
22. Kaneko Y, Sakakibara S, Sanda T, Hashimoto S, submitted to Mater Sci Forum
23. Gale WF, Totemeier TC (2004) Smithells metals reference book. Elsevier, Oxford
24. Bobeth M, Hecker M, Pompe C, Schneider CM, Thomas J, Ullrich J, Wetzig K (2001) Z Metallkd 92:810